Int J Thermophys (2008) 29:1222–1243
DOI 10.1007/s10765-008-0497-7

Viscosity of Imidazolium-Based Ionic Liquids at Elevated Pressures: Cation and Anion Effects

Azita Ahosseini · Aaron M. Scurto

Received: 13 January 2008 / Accepted: 20 July 2008 / Published online: 15 August 2008

Abstract The viscosity of imidazolium-based ionic liquids with four different cations and three different anions was measured to pressures of 126 MPa and at three temperatures (298.15 K, 323.15 K, and 343.15 K). The high-pressure viscosity of 1-ethyl-3-methylimidazolium ([EMIm]), 1-*n*-hexyl-3-methylimidazolium ([HMIm]), and 1-*n*-decyl-3-methylimidazolium ([DMIm]) cations with a common anion, bis(trifluoromethylsulfonyl)imide ($[Tf_2N]$), was measured to determine the alkyl-chain length effect of the cation. An increase in the alkyl-chain length increased the viscosity at elevated pressures. [DMIm] exhibited a larger nonlinear increase with pressure over the shorter alkyl substituents. Anion effects were investigated with [HMIm] as a common cation and anions of $[Tf_2N]$, hexafluorophosphate ($[PF_6]$), and tetrafluoroborate ($[BF_4]$). [HMIm][PF_6], with the highest viscosity, demonstrated a very nonlinear pressure dependence even at relatively moderate pressures (to 30 MPa), similar to the results for [BMIm][PF_6]. A combined Litovitz and Tait equation was utilized to describe the viscosity of the ionic liquids with pressure and temperature and demonstrated good correlation with the experimental data.

Keywords Cation and anion effects · High-pressure viscosity · Imidazolium ionic liquids · Tait equation · Litovitz equation

A. Ahosseini · A. M. Scurto (✉)
Department of Chemical & Petroleum Engineering, University of Kansas,
1530 W. 15th St., 4132 Learned Hall, Lawrence, KS 66045, USA
e-mail: ascurto@ku.edu

A. Ahosseini · A. M. Scurto
NSF-ERC Center for Environmentally Beneficial Catalysis, University of Kansas,
1501 Wakarusa Dr., Suite A 110, Lawrence, KS 66047, USA

1 Introduction

Room-temperature ionic liquids (RTILs) are experiencing focused attention due to their diverse chemistry and potential applications. These low-melting organic salts, which comprise entirely cations and anions, can be molecularly engineered for specific physicochemical properties for use in a variety of fields. It has been estimated that approximately 10^{14} unique cation/anion combinations may exist [1–4]; thus, precise tuning of properties is possible. For example, ionic liquids have been used as absorption media for gases [5,6] and as an extractant in liquid separations [7,8]. As ions, a number of electrochemical applications exist [9–14]. A large variety of reactions may be performed in ILs especially as support media for catalysis and biocatalysis [4,15–20]. ILs may be used for a variety of engineering applications including use as heat transfer fluids [21] and as hydraulic fluids [22].

The measurement of the physicochemical properties of ionic liquids such as viscosity, thermal diffusivity, density, ionic conductivity, and thermal behavior, as well as solubility and polarity, are necessary to understand and utilize these diverse media. An understanding of structural effects on physicochemical properties is important for a rational approach for molecular design of RTILs. Viscosity is an important physical property for a number of processes. For instance, it determines the force and energy required to transfer and mix the ionic liquid with other substances. It appears in many dimensionless groups used in mass- and heat-transfer correlations [23]. Applications that occur at high temperatures and/or pressures require reliable and accurate experimental data and mathematical models. This is especially pertinent for such engineering applications as hydraulic fluids [22]. Ionic liquids cover a wide range of viscosity. For instance, at 283.15 K and ambient pressure, the viscosity of [EMIm][Tf_2N] is 63.6 mPa · s [24], while for [OMIm][PF_6], it is 2.439 mPa · s [25]. This flexibility may be tailored to a particular application; for example, use as a solvent for reactions may require relatively low viscosity, while use as a lubricant or as a supported membrane may require higher viscosity. For comparison, the viscosity of typical organic solvents at ambient conditions covers ranges from 0.2 mPa · s to 10 mPa · s [26].

A large number of models for correlating and predicting the viscosity of pure fluids and mixtures have appeared in the literature. Most of these methods are based on the principle of corresponding states, on the absolute rate theory of Eyring [27], and, more recently, on molecular dynamic calculations [28]. Abbott and coworkers [29–31] used a modified "hole theory" to predict the viscosities of ionic liquids at ambient conditions. The Vogel–Fulcher–Tammann (VFT) equation [32–34] and Litovitz [35,36] equation are empirical equations that have been used, in general, at ambient pressure for liquids with a temperature-dependent flow activation energy.

Crosthwaite et al. [37] measured the viscosity of a number of imidazolium and pyridinium ionic liquids with a cone-and-plate rheometer at ambient pressure. Tokuda et al. [38] investigated the physicochemical properties of several ILs with a fixed 1-butyl-3-methylimidazolium ([BMIm]) cation and different anions: [$(C_2F_5SO_2)_2N$], [$(CF_3SO_2)_2N$] (abbreviated [Tf_2N]), [CF_3SO_3], [PF_6], [CF_3CO_2], and [BF_4] at ambient pressure and various temperatures. [BMIm] with [PF_6] and [$(C_2F_5SO_2)_2N$] produced ILs with a significantly higher viscosity that was attributed to strong coulombic forces among each ionic species in the ionic liquids. Watanabe and coworkers

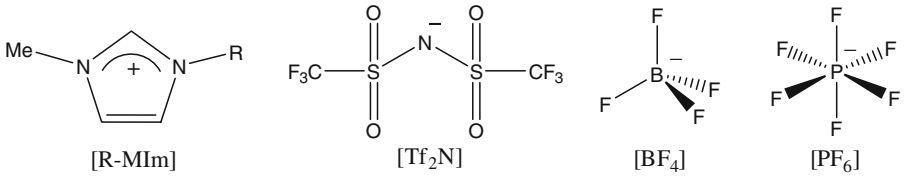

Fig. 1 Structure of methyl imidazolium cations and anions investigated: for [R-MIm], R=ethyl-([EMIm]), *n*-butyl-([BMIm]), *n*-hexyl-([HMIm]), and *n*-decyl-([DMIm])

[39] also carried out similar experiments with different cation classes and a singular anion and determined that an increase in the alkyl chain length of the cation causes an increase in the viscosity. They also demonstrated that imidazolium cations have lower viscosity, higher diffusivity, higher density, and higher thermal stability compared to pyridinium, pyrrolidinium, and ammonium structures [24].

The high-pressure viscosity of ionic liquids has only been measured for a few cation and anion combinations. Harris et al. [25,40,41] measured the viscosity of [BMIm] and [OMIm] [PF_6], and [OMIm][BF_4] with a falling-body viscometer to 353.15 K and approximately 200 MPa. They fitted the data with a modified Litovitz and Vogel–Fulcher–Tammann (VFT) equation to incorporate both temperature and pressure dependences. Kanakubo and coworkers [42] measured the diffusion coefficient and molar conductivity of [BMIm][PF_6] up to 200 MPa and used the Stokes-Einstein equation to back calculate the viscosity. Tomida et al. [43,44] measured the viscosity of similar systems: [BMIm][PF_6], [BMIm][BF_4], [OMIm][PF_6], and [HMIm][PF_6] to moderate pressures (<20 MPa) and at different temperatures. They used the hybrid VFT-Tait equation to correlate the data; *vide infra*.

In this work, the viscosity for several different ionic liquids has been measured under high pressures (up to 126 MPa) and at three temperatures (298.15 K, 323.15 K, and 343.15 K). Both the cation and anion have been systematically altered to investigate the effect of structure on viscosity at elevated pressure. Figure 1 illustrates the cations and anions investigated. The Litovitz equation combined with the Tait equation [45,46] was used to describe the viscosity of ionic liquids as a function of pressure and temperature.

2 Experimental

2.1 Synthesis

2.1.1 General Method

Ionic liquids used in this study were prepared by anion exchange from the corresponding bromide salts of the imidazolium cations with different *n*-alkyl substituents [47,48]. The bromide salt of the imidazolium cation was prepared from a quaternization reaction of 1-methylimidazole with a slight excess amount of the corresponding alkyl bromide in acetonitrile at 313.15 K under an argon atmosphere with stirring for three days. *Caution: These reactions can be highly exothermic and adequate solvent*

volumes and/or cooling must be provided during the reaction. The bromide salts of 1-alkyl-3-methyl-imidazolium were purified with activated charcoal (10 %) stirring for 24 h. Acetonitrile was added to reduce the viscosity of the ionic liquid, and the mixture was filtered. The mixture was then passed through a plug of celite (depth = 7 cm, diameter = 3 cm) and through a short column (height = 20 cm, diameter = 2.5 cm) of acidic alumina. The solvent was removed on a rotary evaporator under a reduced pressure at 313.15 K and then connected to a high vacuum ($<10^{-4}$ torr) at 323.15 K for at least 48 h. The ionic liquids were stored in Schlenk tubes under an atmosphere of dry argon.

2.1.1.1 1-Ethyl-3-Methylimidazolium Bis(Trifluoromethylsulfonyl)Imide ([*EMIm*][*Tf*$_2$*N*]) [EMIm][Tf_2N] was prepared from the anion exchange of [EMIm][Br] with Li[Tf_2N] in deionized water as described in the literature [49]. The denser hydrophobic IL phase is decanted and washed six to eight times with a volume of water approximately twice the volume of the IL. The IL is then dried under vacuum. ^{1}H NMR chemical shifts (relative to TMS internal standard) and coupling constants J/Hz: $\delta = 8.59$ (s, 1H), 7.42(d, 2H, $J = 10.3$), 4.24 (q, 2H, $J = 7.36$), 3.93(s, 3H), 1.54(t, 3H, $J = 7.4$). Analysis calculated for $C_8H_{11}N_3F_6S_2O_4$: C, 24.55; H, 2.83; N, 10.74; S, 16.39. Found: C, 24.62; H, 2.84; N, 10.71; S, 15.88; water content is 24 ppm, and Br content is less than 36 ppm.

2.1.1.2 1-Hexyl-3-Methylimidazolium Bis(Trifluoromethylsulfonyl) Imide ([*HMIm*][*Tf*$_2$*N*]) [HMIm][Tf_2N] was prepared similarly to [EMIm][Tf_2N]. ^{1}H NMR chemical shifts (relative to TMS internal standard) and coupling constants J/Hz: $\delta = 8.65$ (s, 1H), 7.39 (d, 2H, $J = 4.19$), 4.17 (q, 2H, $J = 7.4$), 3.93(s, 3H), 1.87(m, 4H), 1.32(m, 6H) 0.87(t, 3H, $J = 6.53$). Analysis calculated for $C_{12}H_{19}N_3F_6S_2O_4$: C, 32.2; H, 4.28; N, 9.39; S, 14.33. Found: C, 32.21; H, 4.27; N, 9.25; S, 14.19; water content is 125 ppm, and Br content is less than 8 ppm.

2.1.1.3 1-Decyl-3-Methylimidazolium Bis(Trifluoromethylsulfonyl)Imide ([*DMIm*][*Tf*$_2$*N*]) [DMIm][Tf_2N] was prepared similarly to [EMIm][Tf_2N]. ^{1}H NMR chemical shifts (relative to TMS internal standard) and coupling constants J/Hz: $\delta = 8.66$ (s, 1H), 7.36 (s, 1H), 7.36 (s, 1H), 4.15 (t, 2H, $J = 7.5$), 3.92(s, 3H), 1.86(m, 4H), 1.26 (m, 14H), 0.87 (t, 3H, $J = 6.7$). Analysis calculated for $C_{16}H_{27}N_3F_6S_2O_4$: C, 38.17; H, 5.4; N, 8.34; S, 12.73. Found: C, 38.55; H, 5.3; N, 8.15; S, 12.29; water content is 123 ppm, and Br content is less than 53 ppm.

2.1.1.4 1-Hexyl-3-Methylimidazolium Tetrafluoroborate ([*HMIm*] [BF_4]) [HMIm][BF_4] was prepared from the anion exchange of [HMIm][Br] with ammonium tetrafluoroborate in deionized water. ^{1}H NMR chemical shifts (relative to TMS internal standard) and coupling constants J/Hz: $\delta = 8.72$ (s, 1H), 7.52(d, 2H, $J = 3.6$), 4.22 (t, 2H, $J = 7.23$), 3.96(s, 3H), 1.89(m, 4H), 1.32(m, 6H) 0.86(t, 3H, $J = 6.54$). Analysis calculated for $C_{10}H_{19}N_2BF_4$: C, 47.27; H, 7.54; N, 11.02; B, 4.25. Found: C, 46.99; H, 7.21; N, 10.88; B, 4.39; water content is 130 ppm, and Br content is less than 18 ppm.

2.1.1.5 1-Hexyl-3-Methylimidazolium Hexafluorophosphate ([*HMIm*] [PF_6]) [HMIm][PF_6] was prepared from the anion exchange of [HMIm][Br] with ammonium

hexafluorophosphate in deionized water [50,51]. As the [PF_6] anion is known to decompose over time, the compound was tested immediately after synthesis. ^{1}H NMR chemical shifts (relative to TMS internal standard) and coupling constants J/Hz: $\delta = 8.43$ (s, 1H), 7.33(s, 1H), 7.33(s, 1H), 4.12 (t, 2H, $J=7.22$), 3.87(s, 3H), 1.85(m, 4H), 1.28(m, 6H), 0.84 (t, 3H, $J=6.96$). Analysis calculated for $C_{10}H_{19}N_2BF_4$: C, 38.47; H, 6.134; N, 8.97; P, 9.92. Found: C, 38.64; H, 6.01; N, 9.01; P, 9.62; water content is 86 ppm, and Br content is less than 40 ppm.

2.1.1.6 1-Butyl-3-Methylimidazolium Hexafluorophosphate ([*BMIm*] [PF_6]) [BMIm] [PF_6] was prepared in a similar procedure as [HMIm][PF_6], but from the anion exchange of [BMIm][Br] with ammonium hexafluorophosphate in deionized water. As the [PF_6] anion is known to decompose over time, the compound was tested immediately after synthesis. ^{1}H NMR chemical shifts (relative to TMS internal standard) and coupling constants J/Hz: $\delta = 8.35$ (s, 1H), 7.31(s, 1H), 7.28(s, 1H), 4.09 (t, 2H, $J=7.4$), 3.83(s, 3H), 1.79(m, 4H), 1.29(m, 6H), 0.85 (t, 3H, $J=7.4$). Analysis calculated for $C_8H_{15}N_2PF_6$: C, 33.81; H, 5.32;N,9.86; P, 10.90; F,40.11. Found: C, 33.69; H, 5.21; N, 9.63; P, 10.40; F: 41.70; water content is 96 ppm, and Br content is less than 8 ppm.

2.2 Chemical Analysis and Data Analysis

Elemental analysis was performed by Desert Analytics Transwest Geochem. H-NMR spectra were recorded on a Bruker 400 NMR spectrometer using TMS as a reference for H chemical shifts. The water content was determined by a Mettler Toledo DL32 Karl Fischer coulometer and the Br content was measured by a Cole-Parmer bromide electrode (27502-05) read with an Oakton Ion 510 series meter. Data regression was performed with both SigmaPlot 2000-SPSS Inc. and CurveExpert (cvxpt32), which uses the Marquardt-Levenberg algorithm to determine Litovitz and Tait parameters using a sum-of-squares objective function.

2.3 Viscosity Measurement

2.3.1 Apparatus

A Cambridge Applied Systems (currently Cambridge Viscosity, Inc., www.cambridgeviscosity.com) high-pressure viscometer was utilized for these measurements (ViscoPro 2000 System 4-SPL-440 with Viscolab software). A schematic diagram of the apparatus is shown in Fig. 2. The apparatus consists of a temperature-controlled oven (3) (± 0.1 K) which houses the high-pressure viscometer sensor (4). The testing chamber is connected to a rupture disk (RD) (5), a precision pressure transducer (PT) (6), and a resistance temperature detector (RTD) (7). The viscometer was connected to a manual high-pressure syringe pump (2) purchased from High Pressure Equipment Company (HIP) (Model No. 50-575-30; 30,000 psi, capacity of 10 cm^3 with PolyPak).

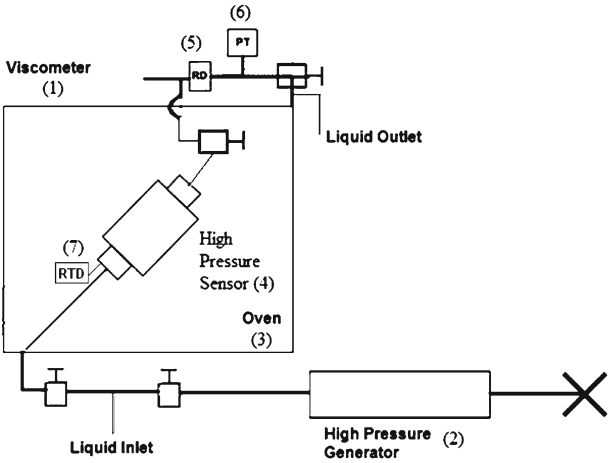

Fig. 2 Schematic of the viscometer apparatus: (1) viscometer, (2) high pressure generator, (3) oven, (4) high pressure sensor, (5) rupture disc, (6) pressure transducer, and (7) RTD temperature probe

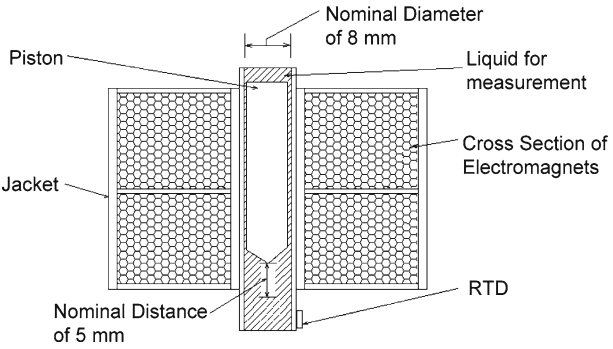

Fig. 3 Features of the Cambridge Viscosity viscometer measurement chamber

The viscometer utilizes the principles of annular flow around an axially oscillating piston [23]. A diagram of the testing chamber is found in Fig. 3 and consists of the chamber, piston, electromagnetic coils, and RTD for temperature measurement. Two magnetic coils inside the sensor body oscillate the piston (one coil at a time) over a fixed distance, forcing the fluid to flow through the annular space between the rod and chamber. One magnetic coil applies a constant force on the piston while the other determines the position of the piston. The roles of the coils reverse when the piston reaches the end of the cycle and changes direction. The time required for the rod to complete a cycle is directly related to the dynamic viscosity of the fluid.

The sensor is capable of measurements from (0.2 to 10,000) mPa · s (cP), at a maximum pressure of 137.9 MPa and in a temperature range of 233.15 K to 463.15 K. Various piston sizes lead to more accurate results over different ranges of viscosity and are changed according to their factory-suggested conditions. As the diameter inside the Inconel 718 chamber slightly increases with pressure, these changes are corrected by a factory-provided conversion equation. The viscosity reading is the

average of 20 viscosity measurements and is reported with the standard deviation of those measurements. The nominal uncertainty of the pressure gauge is 0.07 % full-scale (FS = 206.8 MPa), but the NIST-traceable calibration was accurate to 0.0084 % full-scale. The maximum deviation of temperature from the set-point temperature for all data was 0.1 K, with the average deviation being ±0.07 K.

The viscosity at ambient pressure (at different temperatures) was also measured using a Brookfield DV-III Ultra programmable rheometer to confirm the accuracy of the high-pressure viscometer. The uncertainty of this instrument is ±3 % for the range of viscosity investigated here. The uncertainty of temperature is ±0.1 K.

2.3.2 Measuring Procedure

A volume of approximately (30–40) ml of the dried compound was transferred into the high-pressure manual syringe pump from a Schlenk flask under argon pressure using a stainless steel high-pressure metering pump (Eldex Laboratories, Inc., Model 1020 BBB-4). The water content before and after measurement has been determined, and the maximum amount (after measurement) is reported. The highest deviation of the before and after was 70 ppm. The liquid was forced through the lines to displace any argon pockets. The viscometer has a "purge" feature which rapidly oscillates the rod in the measurement chamber to dislodge any potential bubbles. The ambient pressure viscosity of the ionic liquids was measured and compared with literature results (Table 1).

Table 1 Viscosity η(mPa · s) of ionic liquids at ambient pressure measured by different methods

Reference	[EMIm][Tf_2N]	[HMIm][Tf_2N]	[DMIm][Tf_2N]	[HMIm][BF_4]	[HMIm][PF_6]
$T = 298.15$ K					
[60]					585 (454[a])
[37]	32	68			
[24]	32.6	69.7			
[67]				174.0	
[41]					496.9
This work[b]	34.29 ± 0.1	71.0 ± 0.3	108.2 ± 0.4	202.4 ± 0.8	481.4 ± 2.4
This work[c]	34.1 ± 0.4	71.5 ± 0.8	111.2 ± 1.2	210.4 ± 2.4	489.5 ± 6
$T = 323.15$ K					
[37]	15.0	26.0			
[39]	14.7	24.8			
[24]	15.5	25.8			
[67]				53.9	
[41]					117.0
This work[b]	15.6 ± 0.1	24.9 ± 0.1	36.3 ± 0.1	58.5 ± 0.3	121.4 ± 0.36
$T = 343.15$ K					
[37]	9.0	15.0			
[39]	9.4	13.7			
[24]	9.5	14.1			
[41]					49.7
This work[b]	9.55 ± 0.03	14.1 ± 0.2	18.20 ± 0.05	27.0 ± 0.1	48.1 ± 0.3

[a] Equilibrated with water
[b] Oscillating-piston viscometer
[c] Cone-and-plate viscometer

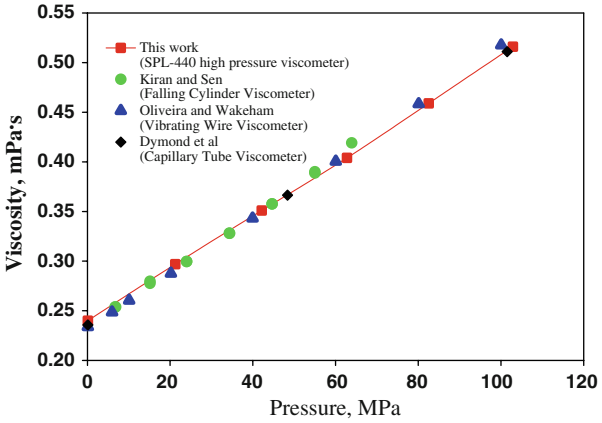

Fig. 4 Effect of pressure on the viscosity of *n*-hexane at 323.15 K (literature: Kiran and Sen [53], Oliveira and Wakeham [54], Dymond et al. [52])

The outlet valve was closed, and the pressure was sequentially increased from 0.1 MPa to 126 MPa. To prevent damage to the viscometer, this pressure was applied at a rate of less than 7 MPa $\cdot$ min^{-1}. The temperatures of interest in this experiment were 298.15 K, 323.15 K, and 343.15 K.

2.3.3 Viscometer Validation

The accuracy of the viscometer was first verified using standard calibration solutions as obtained from the company. The viscosity of n-hexane was measured and compared with high-accuracy literature values [52–54] as shown in Fig. 4. Despite the different experimental methods, e.g., falling-cylinder viscometer, vibrating-wire viscometer, and capillary-tube viscometer, the experimental results here yielded a very high consistency with literature data throughout the large pressure range. Interpolating our data at the pressures measured by each of the different data sets, the percent deviation at each point is plotted in Fig. 5. The nominal reported experimental uncertainty for each of the literature studies is as follows: ± 2 % by Dymond et al. [45] using a capillary-tube method; ± 3 % by Kiran and Sen [53] using a falling-cylinder method; and ± 0.5 % by Oliveira and Wakeham [54] using a vibrating-wire viscometer. As shown in Fig. 5, our data are within the reported uncertainties of Dymond et al. and Kiran and Sen with percent average absolute relative deviation (%AARD) between our interpolated values and the literature values of 0.78 % and 1.1 %, respectively. The % AARD of 1.9 % with the data of Oliveira and Wakeham is outside their reported uncertainty.

2.4 Materials

1-Methyl-imidazole (CAS #616-47-7) 99+ %, acetonitrile $\geq$ 99.9 %, lithium bis (trifluoromethylsulfonyl)imide (CAS #90076-65-6) 99.95 %, ammonium hexafluorophosphate (CAS #16941-11-0) 99.99 %, and ammonium tetrafluoroborate (CAS #13826-83-0) 99.99 % were purchased from Sigma-Aldrich. Bromoethane (CAS# 74-

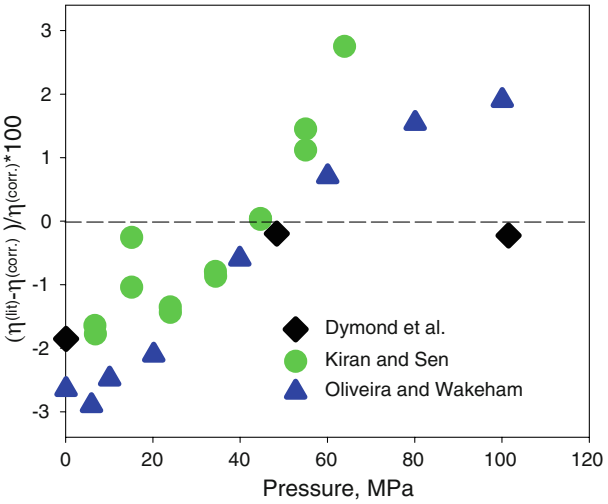

Fig. 5 Deviations of measured viscosities of *n*-hexane at 323.15 K from the literature (literature: Kiran and Sen [53], Oliveira and Wakeham [54], Dymond et al. [52])

96-4) 99+ %, bromobutane (CAS #109-65-9) 99 %, bromohexane (CAS #111-25-1) 99+ %, bromodecane (CAS #112-29-8) 98 %, and aluminum oxide (activated, acidic, for column chromatography; (100–500) micron) were obtained from Acros. The bromo-alkanes and 1-methylimidazole were vacuum distilled directly prior to use. Activated carbon (50–200 mesh) was obtained from Fisher Scientific. Compressed argon (CAS #7440-37-1) (Ultra High Purity (UHP) grade) was obtained from Airgas, Inc.

3 Data Modeling and Analysis

Various theoretical models and empirical expressions can be found in the literature that can be used to represent the viscosity of liquids as functions of pressure and temperature. The variation of viscosity with temperature can be derived in an approximate way from the rate theory approach of Eyring [27], in which the liquids are assumed to have a quasi-crystalline structure [55]. The lattice contains free volume sites that molecules can jump and occupy and make a liquid layer flow with respect to another. The liquid molecules need to pass over a potential energy barrier in order to flow. The height of the barrier, which is equivalent to the flow activation energy, is independent of the temperature, but is influenced by external forces acting on the liquid. The temperature dependence of the viscosity based on the rate theory by the Arrhenius equation [53,55–57] is

$$\ln \eta = \ln A + E/RT \tag{1}$$

where A is a constant, E is the shear flow activation energy, and R is the universal gas constant.

However, few liquids demonstrate an Arrhenius viscosity behavior [58]. The flow activation energy of liquids is temperature-dependent and increases significantly with cooling. Glass forming [59] compounds, which are able to maintain a disordered liquid-like structure below their melting point, often display non-Arrhenius behavior. In these liquids, the viscosity increases strongly with decreasing temperature. Based on these concepts, the Vogel–Fulcher–Tammann (VFT) equation [32–34] is often used, which uses an additional adjustable temperature parameter (T_0) to the exponential term:

$$\ln \eta = \ln A + B(T - C)^{-1} \tag{2}$$

$$\eta = \eta' \exp(B/(T - T_0)) \tag{3}$$

where η' is a pre-exponential factor and B and T_0 are specific adjustable parameters. This equation has been extensively used in the description of cooperative molecular motion in glass-forming and viscous liquids at different temperatures [59]. Most ionic liquids often form glass phases [37,39,60]. Angell [61] has proposed a classification for the fragility of liquids defined as a strength parameter, $D = B/T_0$, based on the VFT equation. According to this definition, strong liquids, where their viscosity approaches the Arrhenius temperature dependence, have a large strength parameter ($D > 30$).

Another empirical equation, which was derived in an approximate way from the rate theory of Eyring, was proposed by Fieggen [55]:

$$\ln \eta = B + A(T - C)^{-1} - D(T - T_1)^2 \tag{4}$$

Fieggen applied this four-parameter equation for liquids such as water, ethanol, toluene, etc. over wide range of temperatures. Fieggen assumed that the thermal expansion is accompanied by an increase of the fraction of unoccupied sites and lattice volume. As in other non-Arrhenius type equations, the height of the potential-energy barrier will depend on temperature (T_1). Litovitz [35,36] has suggested another empirical equation which has been used at ambient pressures:

$$\eta = A \exp(B/RT^3) \tag{5}$$

Harris et al. [25,40] modified both VFT and Litovitz equations to incorporate the temperature and pressure dependence of the viscosity as follows for three pure imidazolium-based ionic liquids:

$$\eta = \exp\{a + bp + (c + dp + ep^2)/T^3\} \tag{6}$$

$$\eta = \exp\{a' + b' + (c' + d' + e'p^2)/(T - T_0)\} \tag{7}$$

In these studies, Harris and coworkers regressed the viscosity of 1-butyl-3-methylimidazolioum hexafluorophosphate [40], 1-methyl-3-octylimidazolium hexafluorophosphate [25], and 1-methyl-3-octylimidazolium tetrafluoroborate [25] between (273.15 and 353.15) K and at pressures to 250 MPa, 176 MPa, and 224 MPa, respectively. They showed that the quality of the fits for both equations is very similar.

The Tait equation is well known to represent the pressure–volume–temperature relationship of many liquids [45,46]. The functional form is

$$\frac{V_0 - V}{PV_0} = \frac{A}{\pi + P} \tag{8}$$

where V_0 and V represent the molar volume at ambient pressure and under pressure P; A and π are constants. Tammann modified the Tait equation [45] to

$$\frac{(V_0 - V)}{V_0} = C \log\left(\frac{B + P}{B + 0.1}\right) \tag{9}$$

The modified equation has become widely accepted to represent high-pressure density data for liquids and liquid mixtures.

In a similar manner, the Tait equation has been used to correlate the pressure dependence of viscosity [46]:

$$\ln\left(\frac{\eta_p}{\eta_o}\right) = E \ln\left(\frac{D + P}{D + 0.1}\right) \tag{10}$$

where η_p and η_0 are the viscosities at a pressure P and at 0.1 MPa, respectively. This equation contains only two fitted parameters and has yielded good correlation with experimental data as shown by Kashiwagi and Makita [46] for aromatic hydrocarbons and cyclohexane up to 110 MPa. Tomida et al. [43,44] have used this equation to correlate the viscosity of [BMIm][PF_6], [BMIm][BF_4], [OMIm][PF_6], and [HMIm][PF_6] at moderate pressures (<20 MPa).

This investigation will utilize a hybrid Tait–Litovitz equation at elevated pressures (to 126 MPa) for the viscosity data for a series of room-temperature ionic liquids:

$$\eta_P = A \exp(B'/T^3)((D + P)/(D + 0.1))^E \tag{11}$$

$$B' = B/R \tag{12}$$

Data at ambient pressure are first correlated using the Litovitz equation, and then the Tait parameters are fitted for the higher pressures. The aforementioned equation has the advantages of containing fewer fitting parameters (A, B, D, E) than other models and simplicity of data analysis. The values of independent parameters, E and D, have been determined as linear functions of temperature (Table 10).

4 Results and Discussion

The viscosity of six methyl-imidazolium-based ionic liquids (see Fig. 1), [HMIm][Tf_2N], [HMIm][PF_6], [BMIm][PF_6], [DMIm][Tf_2N], [EMIm][Tf_2N], and [HMIm][BF_4], has been measured to pressures of approximately 130 MPa. The results are tabulated in Tables 2–7 for temperatures of 298.15 K, 323.15 K, and 343.15 K. The ambient-pressure viscosity for two methods from this work and various literature sources

Table 2 Comparisons of measured viscosities (η) of [BMIm][PF_6] at 298.15 K with literature data (40)

P (MPa)	η (mPa · s)	±SD[a]
0.1	270.9 (273[b])	1
3.4	289.7	2
6.9	305.7	2
12.1	329.2 (329[b])	2
17.2	353.7	1
24.7	396.3 (391[b])	2
25.7	398.2 (390[b])	4
41.4	473.8	1
50.6	543.4 (546[b])	5

[a] SD = standard deviation based on $n = 20$

[b] Data of Harris et al. [40]

Table 3 Measured viscosity (η) of [EMIm][Tf_2N] as a function of pressure and temperature

298.15 K			323.15 K			343.15 K		
P (MPa)	η (mPa · s)	± SD	P (MPa)	η (mPa · s)	± SD	P (MPa)	η (mPa · s)	± SD
0.10	34.4	0.1	0.10	15.6	0.1	0.10	9.6	0.0
2.82	35.0	0.1	2.82	16.1	0.1	2.82	9.8	0.1
4.19	35.3	0.2	4.19	16.4	0.1	4.19	9.9	0.1
7.36	36.2	0.1	7.36	16.9	0.1	7.36	10.2	0.1
35.56	46.8	0.1	35.56	22.0	0.1	35.56	12.6	0.04
48.76	53.3	0.3	48.76	24.9	0.1	48.76	13.8	0.1
69.30	65.0	0.3	69.30	30.8	0.1	69.30	16.0	0.1
85.20	79.4	0.5	85.20	36.7	0.3	85.20	17.7	0.1
96.50	90.0	0.3	96.50	40.1	0.1	96.50	19.2	0.1
110.55	108.6	0.6	110.55	44.8	0.2	110.55	21.2	0.1
122.43	131.5	0.9	121.53	49.5	0.2	125.53	23.4	0.1

Table 4 Measured viscosity (η) of [HMIm][Tf_2N] as a function of pressure and temperature

298.15 K			323.15 K			343.15 K		
P (MPa)	η (mPa · s)	± SD	P (MPa)	η (mPa · s)	± SD	P (MPa)	η (mPa · s)	± SD
0.10	70.96	0.28	0.10	24.9	0.1	0.10	14.07	0.17
2.99	71.04	0.28	2.99	25.81	0.13	2.99	14.12	0.17
4.00	71.38	0.21	4.00	25.98	0.13	4.00	14.22	0.16
7.00	73.71	0.52	7.00	26.87	0.05	7.00	14.6	0.15
35.00	103.4	0.21	35.00	35.96	0.07	35.00	18.62	0.15
50.00	122.2	0.24	50.00	41.57	0.29	50.00	21.1	0.11
70.00	152.2	0.61	70.00	50.43	0.3	70.00	25.17	0.23
83.00	173.2	1.21	83.00	56.96	0.34	83.00	28.12	0.17
93.00	196.3	0.98	93.00	62.11	0.03	93.00	30.42	0.15
110.00	237.6	2.14	110.00	71.6	0.29	110.00	34.65	0.17
124.00	275.7	1.38	124.00	80.46	0.16	124.00	38.34	0.23

Table 5 Measured viscosity (η) of [DMIm][Tf_2N] as a function of pressure and temperature

298.15 K			323.15 K			343.15 K		
P (MPa)	η (mPa·s)	± SD	P (MPa)	η (mPa·s)	± SD	P (MPa)	η (mPa·s)	± SD
0.10	108.2	0.4	0.10	36.2	0.1	0.10	18.15	0.05
2.95	111.5	0.2	2.95	37.5	0.3	2.95	18.55	0.06
4.27	112.8	0.8	4.27	38.2	0.2	4.27	18.75	0.04
6.90	117.6	1.1	6.90	39.2	0.1	6.90	19.30	0.14
34.60	167.5	0.5	34.60	53.6	0.3	34.60	25.76	0.18
47.96	199.0	1.8	47.96	61.8	0.4	47.96	29.15	0.20
68.87	257.0	2.3	68.87	76.0	0.6	68.87	35.72	0.11
83.29	301.1	1.8	83.29	85.9	0.1	83.29	40.47	0.12
93.03	336.7	1.0	93.03	94.3	0.2	93.03	44.56	0.18
109.80	402.7	2.8	109.80	110.8	0.3	109.80	51.26	0.15
122.57	459.8	4.6	122.57	122.6	0.4	122.57	56.74	0.28

Table 6 Measured viscosity (η) of [HMIm][BF_4] as a function of pressure and temperature

298.15 K			323.15 K			343.15 K		
P (MPa)	η (mPa·s)	± SD	P (MPa)	η (mPa·s)	± SD	P (MPa)	η (mPa·s)	± SD
0.10	202	1	0.10	58.5	0.3	0.10	27.0	0.1
2.64	209	3	2.60	59.7	0.1	3.10	27.6	0.1
4.29	213	2	4.13	61.0	0.1	4.10	27.5	0.1
6.95	215	2	6.85	62.0	0.1	7.10	28.0	0.1
34.59	299	2	34.52	79.9	0.2	35.10	35.2	0.3
48.40	387	3	48.18	91.1	0.7	48.34	39.2	0.3
68.14	478	3	68.99	108.2	0.4	68.14	45.0	0.3
82.97	532	3	82.71	121.8	1.1	83.08	49.9	0.2
96.82	621	11	96.55	136.0	0.8	96.55	55.1	0.1
108.55	743	10	110.12	152.4	0.6	110.12	60.8	0.4
117.85	819	12	121.81	165.0	1.3	121.81	65.0	0.4

Table 7 Measured viscosity (η) of [HMIm][PF_6] as a function of pressure and temperature

298.15 K			323.15 K			343.15 K		
P (MPa)	η (mPa·s)	± SD	P (MPa)	η (mPa·s)	± SD	P (MPa)	η (mPa·s)	± SD
0.10	481	2	0.10	121.4	0.4	0.10	48.1	0.3
2.99	523	5	4.00	127.1	0.5	4.00	50.3	0.3
4.00	530	3	7.60	132.4	0.7	7.60	52.0	0.3
7.00	556	4	25.80	164.0	0.7	25.80	62.6	0.2
22.00	701	6	35.00	182.6	0.4	35.00	68.6	0.3
35.00	833	7	50.60	218.9	1.5	50.60	80.5	0.2
42.10	920	8	60.30	241.7	0.7	60.30	88.1	0.4
50.00	1023	8	76.00	280.8	1.1	76.00	102.5	0.4
60.30	1176	5	93.00	334.2	0.3	93.00	118.7	0.6
			101.00	364.2	1.8	101.00	127.1	0.3
			126.00	483.1	1.9	126.00	157.8	0.6

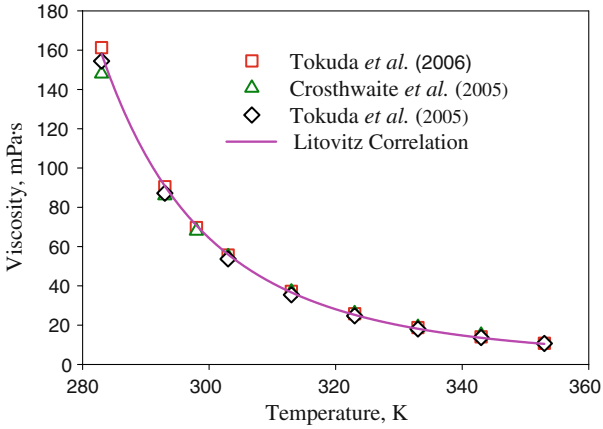

Fig. 6 Effect of temperature on the viscosity of [HMIm][Tf_2N] at atmospheric pressure and comparisons with Tokuda et al. (2006) [24], Crosthwaite et al. (2005) [37], and Tokuda et al. (2005) [39]. Solid line is the Litovitz correlation of the data of this work

are compiled in Table 1. The viscosity of five ionic liquids at 298.15 K was measured using both an ambient-pressure rheometer and the high-pressure viscometer; these data match within a few percent of each other. Both these methods of measurement also correlate well with literature reports. Some of the scatter and deviations among these literature reports may be due to water content, which has been determined to significantly affect viscosity even at low concentrations [62,63]. In addition, the first reported viscosity data for [DMIm][Tf_2N] are given here. Figure 6 depicts the measured viscosity of [HMIm][Tf_2N] with temperature at atmospheric pressure with a comparison of literature data [24,37,39]. This plot illustrates the exponential decrease of viscosity with temperature in a manner consistent with Litovitz behavior. The data presented here show good agreement with several literature data sources as shown in Fig. 7. The literature values seem to be approximately 5 % different from each other; including a roughly 4 % difference from the same research group. Crosthwaite et al. [37] report errors of ±2 %, while Tokuda et al. [39,64] do not state an error range for their data. The viscosity of [BMIm][PF_6] has been measured at elevated pressures at 298.15 K and is illustrated in Fig. 8 and Table 2. A nearly linear trend is observed until approximately 40 MPa, after which the viscosity begins to marginally increase at a faster rate with pressure. While little high-pressure viscosity data for ionic liquids exist in the literature, those of Harris et al. [40] for this system are plotted and excellent agreement (within 0.8 % average absolute relative deviation (%AARD)) is obtained as shown in Fig. 9.

Figures 10 and 11 demonstrate the effect of high pressures at three different temperatures for the viscosity of [HMIm][Tf_2N] and [HMIm][PF_6]. These graphs illustrate that the viscosity at lower temperatures is more sensitive to pressure than at higher temperatures. For instance, for [HMIm][Tf_2N], the viscosity change, from ambient pressure to 124 MPa, is approximately 288.5 % at 298.15 K and 172.5 % at 343.15 K. Thus, the viscosity is more linearly related to pressure at the high temperatures. Figure 11 also

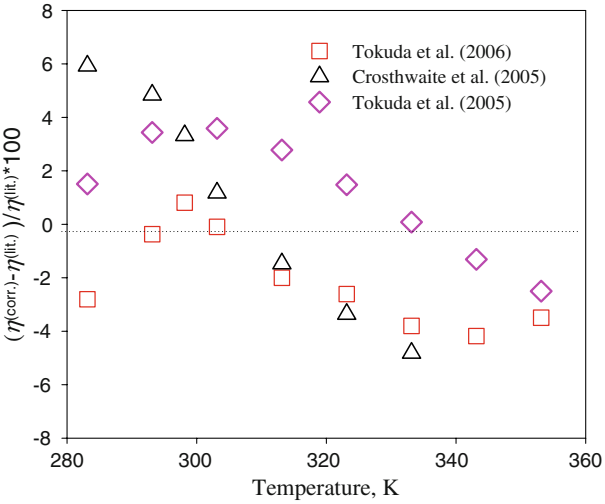

Fig. 7 Deviations of measured viscosities of [HMIm][Tf_2N] at atmospheric pressure from the Litovitz correlation and literature data (Tokuda et al. (2006) [24], Crosthwaite *et al.* (2005) [37], and Tokuda et al. (2005) [39])

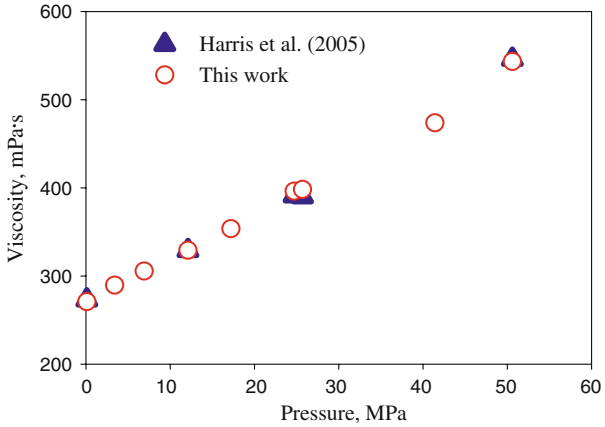

Fig. 8 Effect of pressure on the viscosity of [BMIm][PF_6] at 298.15 K compared with literature data [40]

demonstrates good agreement of the data obtained for the viscosity of [HMIm][PF_6] measured by Harris et al. [41].

A series of experiments were performed to determine the effect of the anion on the high-pressure viscosity using a common cation, 1-hexyl-3-methyl-imidazolium [HMIm]. Three different anions were investigated: [Tf_2N] (Table 4), [BF_4] (Table 6), and [PF_6] (Table 7). Figure 12 illustrates the viscosity of [HMIm] with the three different anions at 298.15 K. The viscosity of [HMIm][PF_6] is considerably higher than that of [HMIm][BF_4] and [HMIm][Tf_2N]. In addition, the rate of increase in viscosity with pressure for [HMIm][PF_6] is much greater than for the other two ionic liquids. While there is not a complete set of physical properties data of these [HMIm] compounds,

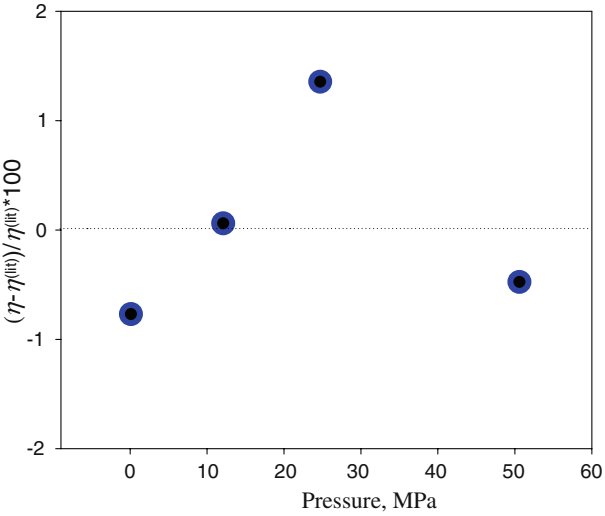

Fig. 9 Deviations of interpolated viscosities of [BMIm][PF_6] at 298.15 K using the Tait–Litovitz equation compared with literature data [40]

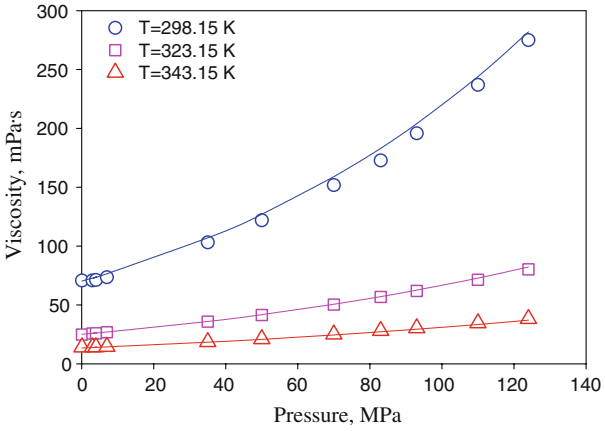

Fig. 10 Viscosity of [HMIm][Tf_2N] at high pressures and different temperatures. All lines, herein, are correlations and predictions from the Tait–Litovitz correlation with parameters from Table 9

Table 8 lists some physical and thermal properties of a similar cation, BMIm, with the anions in question, *viz.*, [Tf_2N], [BF_4], and [PF_6]. The order of increasing viscosity for these three compounds at ambient conditions seems to scale with the melting point (T_m) or, more appropriately, the glass transition temperature (T_g). While this may correlate with the difference in absolute viscosity, it does not predict the larger relative rate of increase with pressure of the [PF_6] anion.

"Hole theory," applied to ILs by Abbott [29–31], indicates that the viscosity of an ionic liquid is inversely related to the size of the molecule. However, with a similar cation, the anionic radius (R_-) increases from [BF_4] < [PF_6] < [Tf_2N] while the

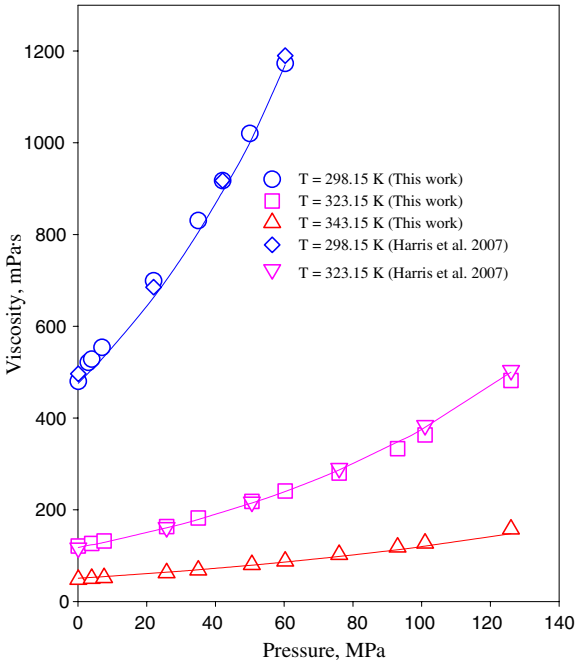

Fig. 11 Viscosity of [HMIm][PF_6] at high pressures and different temperatures compared with Harris et al. [41]

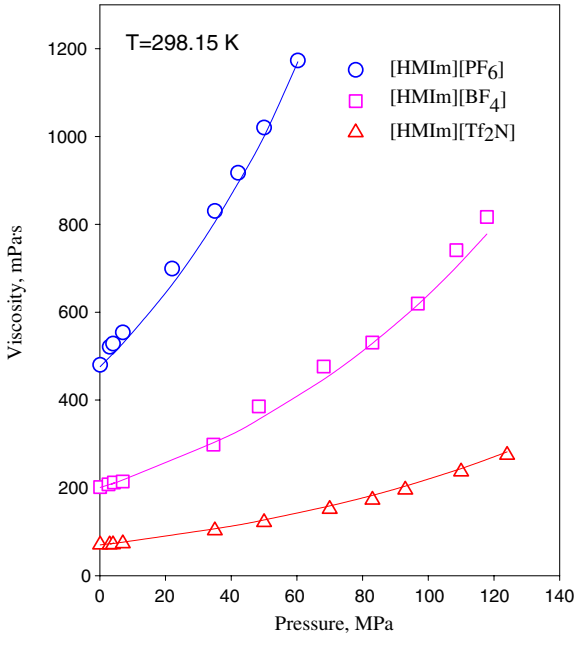

Fig. 12 Viscosity of [HMIm] cations with different anions as a function of pressure at 298.15 K

Table 8 Properties of [BMIm] ionic liquids

Ionic liquid	MW [38] ($g \cdot mol^{-1}$)	T_m [38] (K)	T_g [38]	T_d [38]	R [31] (Å)	V [38] ($cm^3 \cdot mol^{-1}$)	η(298 K) (mPa·s)
[BMIm][Tf_2N]	419.4	270.15	186.15	696.15	3.62	292.4	50.9 [41]
[BMIm][BF_4]	226	N/A	190.15	698.15	2.5	188.7	103.8 [67]
[BMIm][PF_6]	284.2	283.15	196.15	706.15	2.78	208.3	273 [40]

experimental viscosity increases in a mixed order of [Tf_2N] < [BF_4] < [PF_6]; see Table 8. Thus, simple geometric factors such as the radius or hydrodynamic radius do not explain the viscosity behavior of all ionic liquids. Watanabe and coworkers [38] hypothesized that some of the differences observed in the transport properties of the [BMIm] cation and these same anions may be due to different levels of "ionicity" (association/disassociation) that they elucidated from diffusion and ionic conductivity data. [BMIm][PF_6] is believed to have the highest level of dissociation, which may result in a decrease of the free volume. In addition, [BMIm][PF_6] is believed to form a greater number of higher-order aggregates (([BMIm]$_2$[PF_6], [BMIm][PF_6]$_2$, [BMIm]$_2$[PF_6]$_3$, etc.) as determined by mass spectrometry [38]. These aggregates would have larger hydrodynamic radii and extended long-range molecular interactions increasing the barrier to motion. Rebelo and coworkers [65,66] have determined the high-pressure density and isothermal compressibility of these [BMIm] compounds and have found that the isothermal compressibility, κ_T, is relatively small ($<0.53\,GPa^{-1}$) and decreases significantly with pressure. Thus, the density to 100 MPa will increase by less than ~5 %. The [Tf_2N] compound has the highest κ_T, which may indicate a higher free volume and may explain the lowest viscosity despite the larger anion diameter. While the [PF_6] compound has a lower κ_T , the slight increase in density with pressure may induce further aggregation/larger aggregates and viscosity augmentation similar to the results of Watanabe and coworkers [38].

Figure 13 demonstrates the effect of the n-alkyl chain length on the viscosity of methyl-imidazolium cations for a fixed anionic species, [Tf_2N], at high pressures

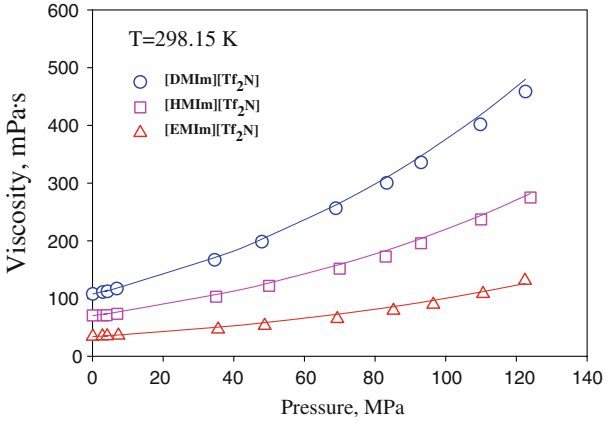

Fig. 13 Pressure dependence of viscosity of [n-alkyl-MIm][Tf_2N] ionic liquids at 298.15 K with correlations

and different temperatures. As this graph illustrates, smaller alkyl chain lengths of the imidazolium cation, such as R = ethyl-, exhibit lower viscosity than the hexyl- or decyl-substituted methylimidazolium cation. In addition, the [DMIm] cation also exhibits a higher rate of change with pressure in the higher pressure regions of the data (>60 MPa).

The viscosity of the RTILs as functions of temperature and pressure is correlated with the Litovitz and Tait equations as discussed above. Table 9 lists the regressed Litovitz and Tait equation parameters for each IL at each of the three different temperatures. The Tait parameters were then correlated to a linear equation and are listed in Table 10. The absolute average relative deviation (AARD%) of the correlated data indicates a good fit between the experimental data and those predicted by the equation. The AARD% of these ionic liquids is in the following order: [HMIm][Tf_2N] = 2.2

Table 9 Tait–Litovitz equation parameters

T (K)	η_0 (mPa·s)	D (MPa)	E
[EMIm][Tf_2N]			
298.15	33.89	871.9	10.0
323.15	15.33	697.9	6.8
343.15	9.50	558.7	4.3
[HMIm][Tf_2N]			
298.15	70.26	553.9	6.9
323.15	25.13	526.1	5.6
343.15	13.51	503.9	4.6
[DMIm][Tf_2N]			
298.15	107.52	388.0	5.5
323.15	35.86	385.2	4.7
343.15	18.49	382.9	4.1
[HMIm][BF_4]			
298.15	200.73	1010.4	12.3
323.15	57.78	678.7	7.1
343.15	27.26	413.3	3.0
[HMIm][PF_6]			
298.15	476.31	1207.3	18.4
323.15	118.22	1080.6	13.1
343.15	51.00	979.3	8.8

Table 10 Tait–Litovitz equation parameters and $\%AARD$[a]

IL	$\eta_0 = A\exp(B'/(T^3))$		$D = a + bT$		$E = c + dT$		$AARD$[a]
	A (mPa·s)	$B' \times 10^{-6}$ (K^3)	a (MPa)	b (MPa·K^{-1})	c	d (K^{-1})	(%)
[EMIm][Tf_2N]	0.8423	97.92	2947	−6.96	48.14	−0.1279	3.9
[HMIm][Tf_2N]	0.583	127	885.13	−1.111	22.03	−0.0508	2.2
[DMIm][Tf_2N]	0.6449	135.6	421.81	−0.1133	14.4	−0.03	2.4
[HMIm][BF_4]	0.6059	153.8	4966.88	−13.27	73.83	−0.2064	4.0
[HMIm][PF_6]	0.7208	172.1	2717.7	−5.066	82.11	−0.2136	3.1

[a] $\%AARD = \frac{100}{N}\sum_{i=1}^{N}\left|\frac{\eta_i^{\text{pred}} - \eta_i^{\text{exp}}}{\eta_i^{\text{exp}}}\right|$

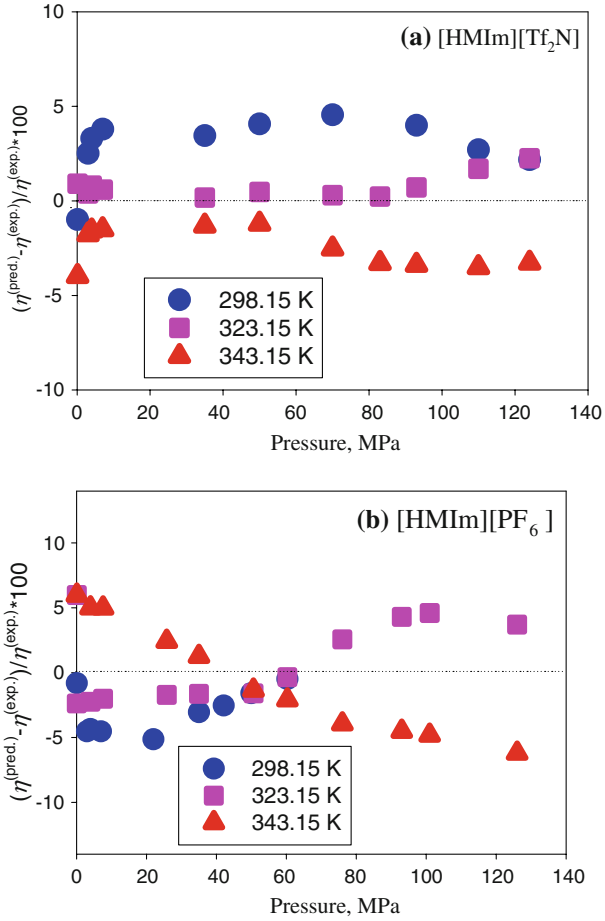

Fig. 14 Deviations of measured viscosities from the Tait-Litovitz equation as a function of pressure and temperature for (**a**) [HMIm][Tf_2N] and (**b**) [HMIm][PF_6]

%, [DMIm][Tf_2N] = 2.4 %, [HMIm][PF_6] = 3.1 %, [EMIm][Tf_2N] = 3.9 %, [HMIm][BF_4] = 4 %. Figure 14 shows graphically the deviations between the experimental and correlated viscosities using the Litovitz-Tait equation as a function of pressure and temperature for [HMIm][Tf_2N] and [HMIm][PF_6], which vary between a maximum of ±8 %. While the deviations for several isotherms at increasing pressure appear systematic (e.g., at 343.15 K for [HMIm][PF_6], a nearly linearly decreasing trend), the majority of the errors for these and other ionic liquids are believed to have more random dependences or bias (e.g., at 298.15 K for [HMIm][Tf_2N]).

5 Summary

The viscosity of a series of pure imidazolium-based RTILs was measured to determine the effect of high pressures (up to 130 MPa) from 298.15 K to 343.15 K with changes

in the cation and anion. The data obtained have an estimated uncertainty of less that 3 % with this high-pressure viscometer and have been shown to have excellent agreement with the small number of literature studies of high-pressure viscosity of ILs. The data have been correlated with a hybrid Litovitz–Tait equation with average absolute relative deviation percentages (AARD%) from 2.2 % for [HMIm][Tf_2N] to 4 % for [HMIm][BF_4].

Acknowledgments This work was supported by the NSF-ERC Center of Environmentally Benign Catalysis (CEBC EEC-0310689) and the National Science Foundation (NSF CBET-0731244). We would like to kindly thank Dr. W. Kirk Snavely for aiding in the setup of the viscometer. We would also like to thank Mr. Christopher Sharpe for some experimental assistance. The primary reviewer is kindly thanked for careful reading and helpful suggestions.

References

1. S.A. Forsyth, J.M. Pringle, D.R. MacFarlane, Aus. J. Chem. **57**, 113 (2004)
2. J.S. Wilkes, J. Mol. Cat. A **214**, 11 (2004)
3. L. Ropel, L.S. Belveze, S. Aki, M.A. Stadtherr, J.F. Brennecke, Green Chem. **7**, 83 (2005)
4. A. Ahosseini, W. Ren, A. Scurto, Chem. Today/Chim. Oggi **25**, 40 (2007)
5. L.A. Blanchard, D. Hancu, E.J. Beckman, J.F. Brennecke, Nature **399**, 28 (1999)
6. C. Cadena, J.L. Anthony, J.K. Shah, T.I. Morrow, J.F. Brennecke, E. J. Maginn, J. Am. Chem. Soc. **126**, 5300 (2004)
7. A.G. Fadeev , M.M. Meagher, Chem. Comm. 295 (2001)
8. A.E. Visser, R.P. Swatloski, W.M. Reichert, S.T. Griffin, R.D. Rogers, Ind. Eng. Chem. Res **39**, 3596 (2000)
9. B.M. Quinn, Z. Ding, R. Moulton, A.J. Bard, Langmuir **18**, 1734 (2002)
10. J.S. Wilkes, J.A. Levisky, R.A. Wilson, C.L. Hussey, Inorg. Chem. **21**, 1263 (1982)
11. F. Endres, ChemPhysChem **3**, 144 (2002)
12. J. Fuller, R.T. Carlin, R.A. Osteryoung, J. Electrochem. Soc. **144**, 3881 (1997)
13. J. Fuller, A.C. Breda, R.T. Carlin, J. Electroanal. Chem. **459**, 29 (1998)
14. W. Lu, A.G. Fadeev, B. Qi, E. Smela, B.R. Mattes, J. Ding, G.M. Spinks, J. Mazurkiewicz, D. Zhou, G.G. Wallace, Science **297**, 983 (2002)
15. Y. Chauvin, L. Mussmann, H. Olivier, Angew. Chem. Int. Ed. **34**, 2698 (1995)
16. U. Kragl, M. Eckstein, N. Kaftzik, Curr. Opin. Biotech. **13**, 565 (2002)
17. P. Lozano, T. De Diego, D. Carrié, M. Vaultier, J.L. Iborra, Biotech. Lett. **23**, 1529 (2001)
18. R.A. Sheldon, R. M. Lau, M.J. Sorgedrager, F. van Rantwijk, K.R. Seddon, Green Chem. **4**, 147 (2002)
19. T. Welton, Chem. Rev. **99**, 2071 (1999)
20. D. Zhao, M. Wu, Y. Kou, E. Min, Catal. Today **74**, 157 (2002)
21. M.E. Van Valkenburg, R.L. Vaughn, M. Williams, J.S. Wilkes, Thermochim. Acta **425**, 181 (2005)
22. V.R. Koch, C. Nanjundiah , R.T. Carlin, U.S. Patent No. 5,827,602, Oct. 27, 1998
23. R.B. Bird, W.E. Stewart, E.N. Lightfoot, *Transport Phenomena* (Wiley, New York, 1960)
24. H. Tokuda, K. Ishii, M. Susan, S. Tsuzuki, K. Hayamizu, M. Watanabe, J. Phys. Chem. B **110**, 2833 (2006)
25. K.R. Harris, M. Kanakubo, L.A. Woolf, J. Chem. Eng. Data **51**, 1161 (2006)
26. M.S. Kelkar, E.J. Maginn, J. Phys. Chem. B **111**, 4867 (2007)
27. S. Glasstone, K.J. Laidler, H. Eyring, *The Theory of Rate Processes* (McGraw-Hill, New York, 1941)
28. M.S. Kelkar, E.J. Maginn, J. Phys. Chem. B **111**, 4867 (2007)
29. A.P. Abbott, G. Capper, S. Gray, ChemPhysChem **7**, 803 (2006)
30. A.P. Abbott, ChemPhysChem **6**, 2503 (2005)
31. A.P. Abbott, ChemPhysChem **5**, 1242 (2004)
32. H. Vogel, Phys. Z **22**, 645 (1921)
33. G.S. Fulcher, Am. Ceram. Soc. J. **8**, 339 (1925)
34. G. Tammann, W. Hesse, Z. Anorg. Allg. Chem. **156**, 245 (1926)
35. T.A. Litovitz, J. Chem. Phys. **20**, 1088 (1952)

36. T.A. Litovitz, J. Chem. Phys. **20**, 1980 (1952)
37. J.M. Crosthwaite, M.J. Muldoon, J.K. Dixon, J.L. Anderson, J.F. Brennecke, J. Chem. Thermodyn. **37**, 559 (2005)
38. H. Tokuda, K. Hayamizu, K. Ishii, M. Susan, M. Watanabe, J. Phys. Chem. B **108**, 16593 (2004)
39. H. Tokuda, K. Hayamizu, K. Ishii, M. Susan, M. Watanabe, J. Phys. Chem. B **109**, 6103 (2005)
40. K.R. Harris, L.A. Woolf, M. Kanakubo, J. Chem. Eng. Data **50**, 1777 (2005)
41. K.R. Harris, M. Kanakubo, L.A. Woolf, J. Chem. Eng. Data **52**, 1080 (2007)
42. M. Kanakubo, K.R. Harris, N. Tsuchihashi, K. Ibuki, M. Ueno, J. Phys. Chem. B **111**, 2062 (2007)
43. D. Tomida, A. Kumagai, K. Qiao, C. Yokoyama, Int. J. Thermophys. **27**, 39 (2006)
44. D. Tomida, A. Kumagai, S. Kenmochi, K. Qiao, C. Yokoyama, J. Chem. Eng. Data **52**, 577 (2007)
45. J.H. Dymond, R. Malhotra, Int. J. Thermophys. **9**, 941 (1988)
46. H. Kashiwagi, T. Makita, Int. J. Thermophys. **3**, 289 (1982)
47. P. Bonhôte, A.P. Dias, N. Papageorgiou, K. Kalyanasundaram, M. Gratzel, Inorg. Chem. **35**, 1168 (1996)
48. A.K. Burrell, R.E.D. Sesto, S.N. Baker, T.M. McCleskey, G.A. Baker, Green Chem. **9**, 449 (2007)
49. P. Nockemann, K. Binnemans, K. Driesen, Chem. Phys. Lett. **415**, 131 (2005)
50. T. Maruyama, S. Nagasawa, M. Goto, Biotech. Lett. **24**, 1341 (2002)
51. B. Wang, Y.R. Kang, L.M. Yang, J.S. Suo, J. Mol. Catal. A **203**, 29 (2003)
52. J.H. Dymond, K.J. Young, J.D. Isdale, Int. J. Thermophys. **1**, 345 (1980)
53. E. Kiran, Y.L. Sen, Int. J. Thermophys. **13**, 411 (1992)
54. C.M.B.P. Oliveira, W.A. Wakeham, Int. J. Thermophys. **13**, 773 (1992)
55. W. Fieggen, Recl. Trav. Chim. Pay. B **89**, 625 (1970)
56. H.S. Ray, S. Pal, Ironmak. Steelmak. **31**, 125 (2004)
57. Y. Xiong, E. Kiran, Polymer **38**, 5185 (1997)
58. J.C. Dyre, T. Christensen, N.B. Olsen, J. Non-Cryst. Solids **352**, 4635 (2006)
59. J.F. Mano , E. Pereira, J. Phys. Chem. **108**, 10824 (2004)
60. J.G. Huddleston, A.E. Visser, W.M. Reichert, H.D. Willauer, G.A. Broker, R.D. Rogers, Green Chem. **3**, 156 (2001)
61. C. Angell, J. Phys. Chem. Solids **49**, 863 (1988)
62. K.R. Seddon, A. Stark, M.J. Torres, Pure Appl. Chem. **72**, 2275 (2000)
63. J.A. Widegren, A. Laesecke, J.W. Magee, Chem. Commun. 1610 (2005)
64. H. Tokuda, K. Ishii, M. Susan, S. Tsuzuki, K. Hayamizu, M. Watanabe, J. Phys. Chem. B **110**, 2833 (2006)
65. R. Gomes de Azevedo, J.M.S.S. Esperança, V. Najdanovic-Visak, Z.P. Visak, H.J.R. Guedes, M. Nunes da Ponte, L.P.N. Rebelo, J. Chem. Eng. Data **50**, 997 (2005)
66. R. Gomes de Azevedo, J. Esperança, J. Szydlowski, Z.P. Visak, P.F. Pires, H.J.R. Guedes, L.P. N. Rebelo, J. Chem. Thermodyn. **37**, 888 (2005)
67. Y.A. Sanmamed, D. González-Salgado, J. Troncoso, C.A. Cerdeiriña, L. Romaní, Fluid Phase Equilib. **252**, 96 (2007)